Aeronautical Research Institute, University of Tokyo
Report No. 391, March 1964

Studies of High Frequency Combustion Oscillations in a Gaseous Propellant Rocket Motor

By

Hiroshi TSUJI and Tadao TAKENO

Summary. The experimental studies were conducted in a research rocket motor burning premixed gases as propellants for investigating the effects of several variables upon the high frequency combustion oscillations in a rocket motor in detail and making clear the driving mechanism of these oscillations. The effects of the combustion chamber length, the propellant equivalence ratio, the mean chamber pressure and the shape of the nozzle upon the longitudinal-mode pressure oscillations were examined. The research rocket motor had a rectangular combustion chamber of 5 cm×8 cm cross section and the propellants used were the premixed city gas and air.

Three modes of the longitudinal pressure oscillations, namely, the fundamental-, the second harmonic- and the third harmonic-mode oscillations were observed in the combustion chamber and the measured periods of each mode oscillation were found to satisfy the relation of acoustic-mode oscillations. Therefore the high frequency combustion pressure oscillations may be treated essentially as the standing waves of the longitudinal mode, though the propagating shock-type pressure waves appeared as the feed energy to the oscillation was increased.

The fundamental- and the higher harmonic-mode pressure oscillations occurred only for certain conditions of the chamber length, the propellant equivalence ratio and the chamber pressure. With increasing the chamber length and the chamber pressure, the instability regions of each mode oscillation were increased. It was confirmed from the experimental results of the instability regions that the combustion oscillations are initiated and sustained only when the period of the oscillation is larger than some combustion time lag determined by the chamber pressure, the fuel compositions, the mixture ratio, the injection velocity of propellant, etc.

I. INTRODUCTION

The combustion in a liquid-propellont rocket motor is never perfectly smooth and is usually accompanied with the pressure fluctuations. In certain cases, these fluctuations may become organized oscillations with well-defined frequencies, being driven by some mechanism which is closely related to the combustion process in the motor. The problem of combustion oscillations is a very serious one, because the pressure oscillations may cause not only a large increase in the heat transfer to the combustion chamber wall but also severe structural damages to the rocket motor.

As is well known, the combustion oscillations can be classified into two ranges of frequencies, low frequencies and high frequencies. Many theoretical analyses and experimental works have been carried out to investigate the low frequency

This document is provided by JAXA.

combustion oscillations and this type of oscillations has been found to be closely associated with the dynamic characteristics of the propellant feed system. On the other hand, the high frequency combustion oscillations have also been extensively analyzed but have proved to be more complex in phenomena than the low frequency combustion oscillations. Mechanisms and theoretical formulations based on these mechanisms have been proposed to explain the phenomena of high frequency combustion oscillations.

The important experimental works on the high frequency combustion oscillation in a liquid-propellant rocket motor were carried out by K. Berman, S. E. Logan and S. H. Cheney, Jr. [*1*] [*2*] [*3*], and independently by H. Ellis and his group [*4*]. In their experiments, a cylindrical combustion chamber with a slit window was used, and the detailed photographic investigations of the combustion process and the simultaneous pressure measurements were made. They all were concerned with the longitudinal-mode oscillations. The main characteristics of the oscillations observed in their experiments can be summarized as follows: 1. The pressure waves propagate back and forth in the combustion chamber. 2. These pressure waves may be sinusoidal-type waves of small amplitudes, or may in certain conditions become shock-type waves of large amplitudes. 3. The observed frequencies of the pressure oscillations are closely associated with the fundamental acoustic mode in the combustion chamber with both ends closed. 4. There is a lower critical chamber length below which no high frequency oscillations appear, and with increase of the chamber length, the oscillations become more severe. K. Berman and S. H. Cheney, Jr. suggested a mechanism to explain some of the phenomena they observed [*2*] [*3*], but their suggestion seems to be inadequate.

Recently, experimental studies of the transverse acoustic modes of the combustion oscillations in a rocket motor were made by P. B. Lawhead with a two-dimensional research thrust chamber which was designed to make extensive use of photographic techniques for observing the combustion and fluid dynamic processes inside the operating thrust chamber [*5*]. Although the amplitude of the pressure oscillations was large, the observed frequency of the transverse pressure oscillation was found to be just the frequency which is predicted from the classical small-amplitude theory.

L. Crocco and S. I. Cheng studied the combustion instability in liquid-propellant rocket motors theoretically. They introduced an idea of time lag which was defined as the time elapsed between the injection of a propellant element and its sudden conversion into hot gases. In their analysis, they substituted this time lag for the complex combustion phenomenon and thus simplified the problem. With this approximation, they developed a linear theory of combustion oscillations through the method of small perturbations [*6*]. Based on Crocco's sensitive combustion time lag theory, L. Crocco, J. Grey and D. T. Harrje made a theoretical formulation of the longitudinal high frequency rocket instability criteria by a considerably simpler but somewhat less rigorous derivation and compared the theoretical instability limit with their experimental results [*7*]. Another theo-

This document is provided by JAXA.

retical analysis on the instability of high frequency pressure oscillations in rocket combustion chambers was made recently by F. E. C. Culick [*8*]. By emphasizing the energy addition by combustion, he developed an analysis for the stability of stationary pressure waves in combustion chambers. The formulation was for the three-dimensional case and the computations were carried out in detail for a cylindrical chamber in which the mean velocity is parallel to the axis and varies only with axial position. It is noteworthy, however, that, because of our meagre knowledge concerning the physico-chemical processes of combustion in a liquid-propellant rocket motor, any analytical approach to the combustion oscillations must start with some hypothetical simple model.

Many studies on the high frequency combustion oscillations have also been made to understand the screech phenomenon observed in turbojet engine afterburners and ramjet combustors [*9*]. This oscillation was found to be closely associated with acoustic mode in the chamber, but it is clearly evident that the driving mechanism for the screech will differ markedly from those for the oscillations in the rocket motor [*5*] [*9*]. On the other hand, independently of the combustion oscillations in a rocket motor and a jet engine, the phenomenon of flame-driven oscillations of gas flows has been known for a long time as singing flame. About this problem, there are excellent experimental works by A. A. Putnam and W. R. Dennis [*10*]~[*14*] and a series of detailed theoretical analyses by M. J. Merk [*15*]~[*19*].

Recently, a series of experimental investigations of some of the factors affecting the high frequency combustion pressure oscillations has been carried out by M. J. Zucrow, J. R. Osborn, et al. with a cylindrical rocket motor burning premixed gases as the propellants [*20*]~[*24*]. By employing such a relatively simple combustion system of premixed gases, the experimental work is simplified, and the effects of several of the variables which enter into the combustion process for a liquid-propellant rocket motor, such as mixing, atomization, vaporization, etc. are eliminated. These experimental results afford interesting comparison with those observed with liquid propellants. The main characteristics of the combustion oscillations observed in the gaseous propellant rocket motor are as follows: 1. The longitudinal-mode pressure oscillations or/and the transverse-mode pressure oscillations are observed in the combustion chamber. 2. These pressure waves may be sinusoidal-type waves of small amplitudes, or may in certain conditions become shock-type waves of large amplitudes. 3. The instability regions for the transverse-mode oscillations progress steadily toward higher chamber pressure with increasing chamber length, and the amplitudes of these oscillations decrease as the chamber length increases at a fixed chamber pressure. 4. The amplitudes of the longitudinal-mode oscillations decrease with decreasing chamber length, and there exists a lower critical combustion chamber length below which no high frequency combustion pressure oscillations of a longitudinal mode occur. The observed frequencies of these oscillations are inversely proportional to the chamber length.

It is easily understood from these experimental results that the high frequency

This document is provided by JAXA.

combustion oscillation observed in a rocket motor burning premixed gases as propellants have much the same character as when the propellants are initially in liquid form. Therefore it is suggested that the essential features of the combustion oscillations can be studied in the simplified conditions by using the premixed gaseous propellants instead of the liquid propellants. Both of the oscillations occurred in the liquid-propellant motor and in the gaseous propellant motor are heat-driven oscillations, and excitation of oscillations may be attributed to the response of the heat source to the disturbances to the gas flow.

Independently of the experiments conducted at the Purdue University, an experimental study on the high frequency combustion oscillations has also been conducted at our Institute by using premixed gaseous propellants, with the object of investigating the effects of the several variables upon the combustion oscillations in a rocket motor in detail and of making clear the driving mechanism of these oscillations. The experiment which is described in this paper was carried out with a rocket motor of rectangular cross section. Premixed city gas and air were used as propellants. The effects of the length of the combustion chamber, the propellant equivalence ratio, the mean chamber pressure and the shape of the nozzle upon the combustion oscillations were examined. In this paper, the experimental results of the longitudinal-mode combustion pressure oscillations are presented and a mechanism of initiating the combustion oscillations is proposed to explain some of the results obtained in the present experiment.

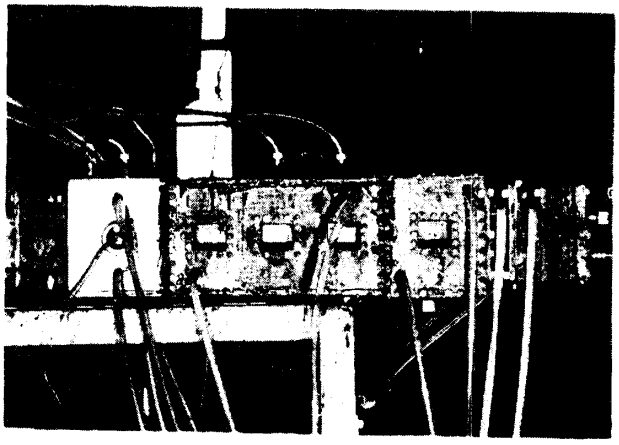

FIGURE 1. Photograph of research rocket motor.

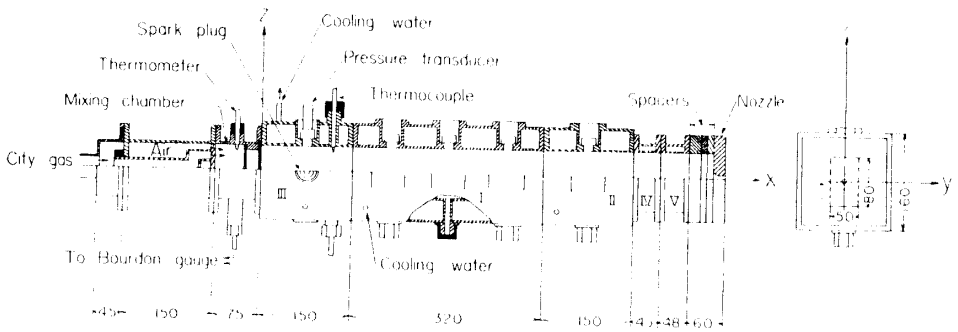

FIGURE 2. Research rocket motor.

This document is provided by JAXA.

II. Experimental Apparatus

The present experiment was conducted utilizing the research rocket motor shown in Figure 1. Figure 2 presents a cross-sectional drawing of the motor. The motor had a rectangular combustion chamber of 5 cm × 8 cm internal cross section and it was composed of a mixing chamber, five water-cooled combustion chamber sections, three uncooled spacers and a nozzle. The lengths of these chamber sections were 32.0 cm, 15.0 cm, 15.0 cm, 4.5 cm and 4.8 cm for chamber sections No. I, No. II, No. III, No. IV and No. V, respectively. The sides of chamber sections No. I and No. II were fitted with 10 mm thick quartz windows to permit viewing and photographing the combustion process in the chamber. The thickness of the spacer was 1 cm or 2 cm. The length of the combustion chamber was varied from 15.0 cm to 75.3 cm by combining these chamber sections and spacers.

The propellants used were the premixed city gas and air and introduced continuously into the combustion chamber through the supplying system shown in Figure 3 [*25*] [*26*]. The air was supplied from a two-stage rotary compressor through

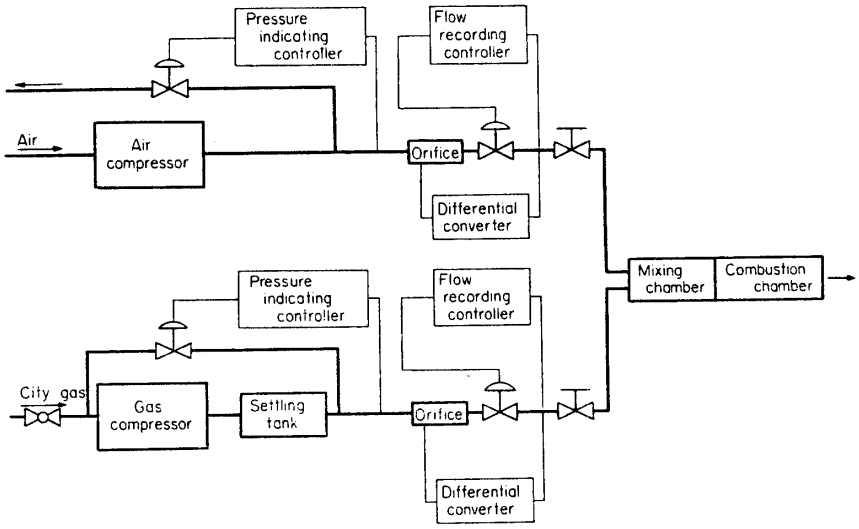

FIGURE 3. Schematic diagram of supplying system.

coolers, purifiers, an orifice and a control valve to the mixing chamber. The city gas was fed by a reciprocating compressor through a cooler, a settling tank, an orifice and a control valve to the mixing chamber. The flow rates of the air and the gas were metered separately by calibrated orifices and controlled by the pneumatic control valves installed in the respective feed lines. The average composition of the city gas was about CO_2, 9.0; O_2, 2.8; CO, 6.2; H_2, 37.0; CH_4, 24.0; C_2H_4, 4.0; C_3H_6, 4.0; N_2, 13.0 per cent. The stoichiometric gas-air ratio of the city gas was found as 1:4.33 and the equivalence ratio of the mixtures was calculated on this basis.

The city gas and the air were introduced into the mixing chamber, impinging on each other, and then mixed thoroughly. The premixed gas entered into the injection section of the mixing chamber through a choked orifice. This choked orifice was installed so as to suppress any low frequency combustion pressure

This document is provided by JAXA.

oscillation to occur and also to prevent the upstream propagating flame in the case of flash back. A cross-sectional drawing of the mixing chamber and the choked orifice is illustrated in Figure 4. The premixed gas was injected into the combustion chamber through a injector which had 20 small holes drilled parallel to the motor axis. The distribution of the injection holes is also shown in Figure 4.

Two types of converging nozzles were used in the present experiment (Figure

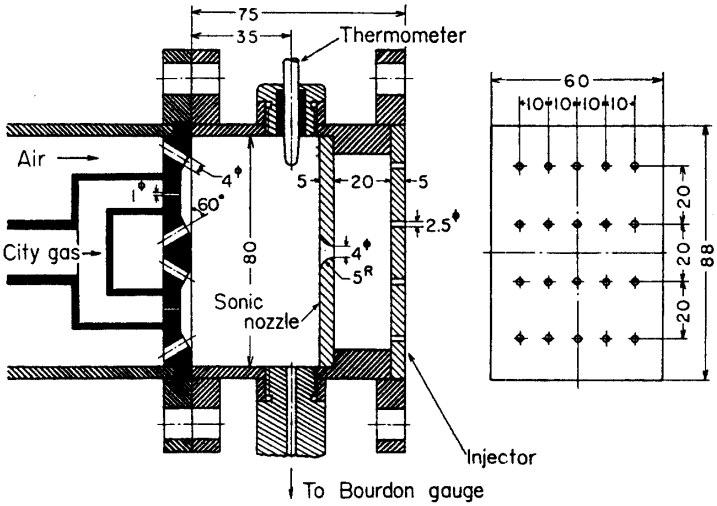

FIGURE 4. Mixing chamber and injector.

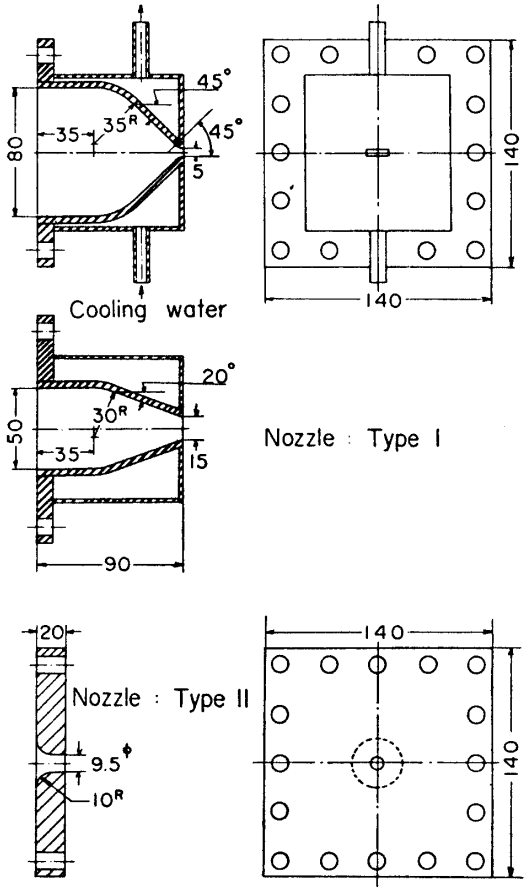

FIGURE 5. Converging nozzle configurations.

This document is provided by JAXA.

5). The nozzle of Type I was water-cooled and had a conventional converging profiles with the throat of 5 mm × 15 mm cross section. The nozzle of Type II was an uncooled flat plate of 20 mm thickness with a circular throat of 9.5 mm diameter. Most of the experiments were carried out with the nozzle of Type II in order to avoid the complex reflection of the pressure waves at the entrance section of the nozzle end.

The mean pressures in the mixing chamber and in the combustion chamber were measured with Bourdon gauges. The temperatures of the combustion gas in the combustion chamber were measured with Pt-Pt.Rh thermocouples jutting 17 mm into the chamber from the upper wall. The pressure oscillations in the combustion chamber were measured with water-cooled strain-gauge type pressure transducers (KYOWA MUSEN PHF-3D; natural frequency is 40 kcps) mounted flush with the chamber wall and their associated electrical equipments (KYOWA MUSEN PM-10N Monitor). The transducers were calibrated statically and their dynamic frequency characteristics were examined by the shock tube test. The noise of the exhaust gas from the motor was picked up by a ribbon microphone (AIWA VM-18; frequency range, 6 cps-10 kcps) placed at about one meter downstream of the nozzle. The electrical outputs of the transducers and the microphone were fed into a synchroscope (IWASAKI SS-5032) and recorded on films.

III. Experimental Results

Most of the measurements were made with a transducer mounted at a position of 7.5 cm from the injector face and a thermocouple fixed at a positon of 12 cm from the injector face as shown in Figure 2. For various lengths of the combustion chamber, the instability regions for the combustion pressure oscillations were determined by varying the propellant equivalence ratio φ and the mean chmber pressure P_c. In the case in which the oscillations occurred, it was found that the oscillating pressure in the combustion chamber and the noise of the exhaust gas had the identical oscillation period although they had different wave forms and phases. Therefore the instability boundaries were determined by hearing the noise of the exhaust gas and confirmed by the pressure traces on the synchroscope. The amplitude and the period of the pressure oscillations were measured from the pressure traces recorded on films.

III-1. Classification of the Pressure Oscillation

In the present experiment three modes of the longitudinal pressure oscillations were observed. They are the fundamental-, the second harmonic- and the third harmonic-modes. Their tyical wave forms are illustrated in Figures 6 and 7. Each mode of the pressure oscillation occurred only in certain conditions of the chamber length, the propellant equivalence ratio and the chamber pressure.

The combustion pressure oscillations of the longitudinal mode have been classified into two principal categories called for convenience the "sinusoidal" type and the "shock" type [*10*]. Also in the present experiment, these two types of

This document is provided by JAXA.

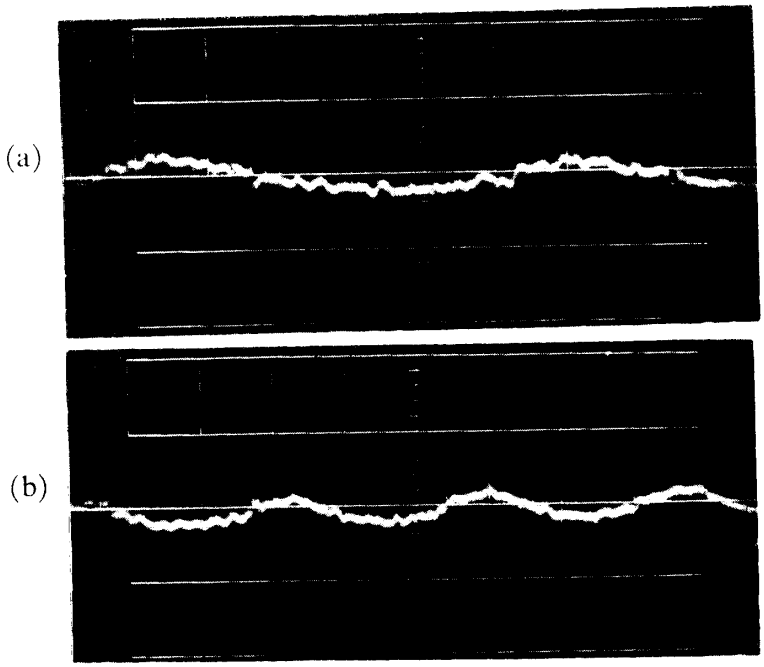

FIGURE 6. Pressure traces of sinusoidal-type oscillations: $L_c = 75.3$ cm.
(a) Fundamental-mode, $P_c = 2.20\,\mathrm{kg/cm^2}$ abs. 500μsec/div.
(b) Second harmonic-mode, $P_c = 2.20\,\mathrm{kg/cm^2}$ abs. 500μsec/div.

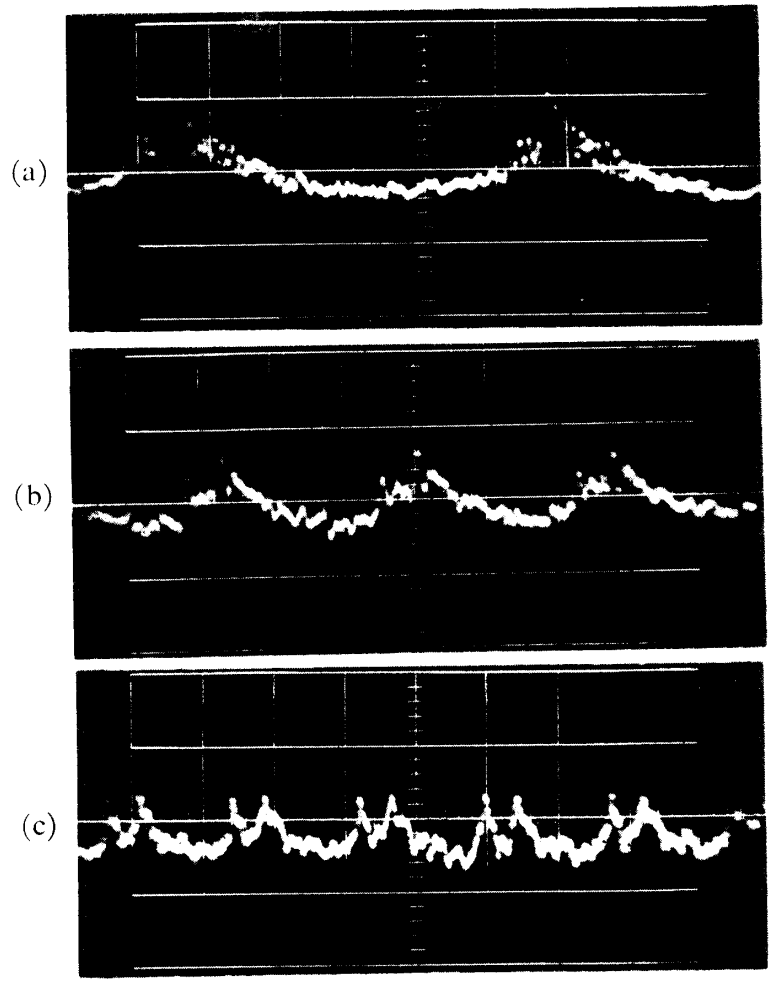

FIGURE 7. Typical pressure traces of shock-type oscillations: $L_c = 75.3$ cm.
(a) Fundamental-mode, $P_c = 2.35\,\mathrm{kg/cm^2}$ abs. 500μsec/div.
(b) Second harmonic-mode, $P_c = 2.30\,\mathrm{kg/cm^2}$ abs. 500μsec/div.
(c) Third harmonic-mode, $P_c = 3.20\,\mathrm{kg/cm^2}$ abs. 500μsec/div.

This document is provided by JAXA.

pressure oscillations were observed. In the case of lower chamber pressure, the smooth sinusoidal wave forms of the oscillations with small amplitudes were observed as shown in Figure 6, and therefore these waves seem to be the standing waves.

As the chamber pressure and the combustion gas temperature were increased, the amplitudes of the pressure oscillations increased and finally the shock-type pressure oscillations appeared as shown in Figure 7. The extreme rapid rise in pressure at the beginning of each cycle of this oscillation is quite similar to that for a normal shock wave. It can be seen that the overall pressure rise comprised two rapid increases in pressure. The first pressure rise occurred when a longitudinal pressure wave propagating toward the injector passed the pressure transducer and the second pressure rise was due to the same pressure wave passing the pressure transducer after being reflected from the injector face. It was found that, for a given chamber length, the time elapsed between these two rapid pressure rises appeared in each cycle of the oscillation was approximately equal for the fundamental-, the second harmonic- and the third harmonic-mode oscillation in the case in which the combustion gas temperature was about the same.

III-2. Effect of the Chamber Length

(*A*) *Longitudinal-mode instability regions*

Figures 8～15 present some of the results on the instability regions determined for each chamber length in the case in which the chamber length L_c was varied

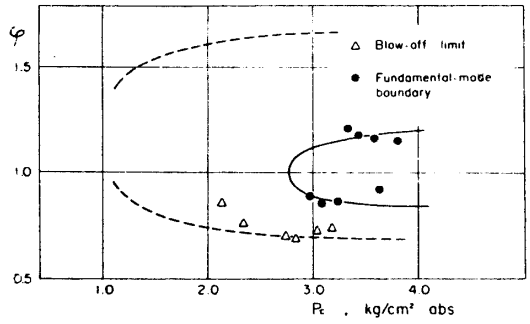

FIGURE 8. Instability region: L_c=19.5 cm.

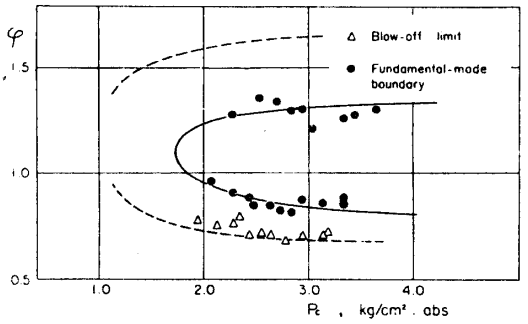

FIGURE 9. Instability region: L_c=22.5 cm.

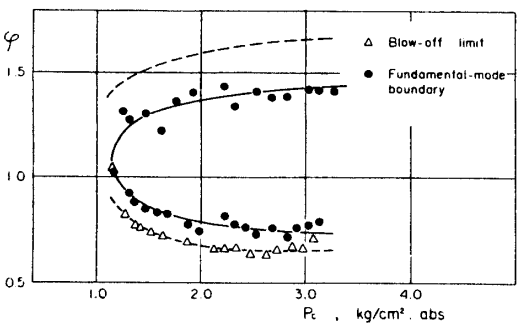

FIGURE 10. Instability region: L_c=30.0 cm.

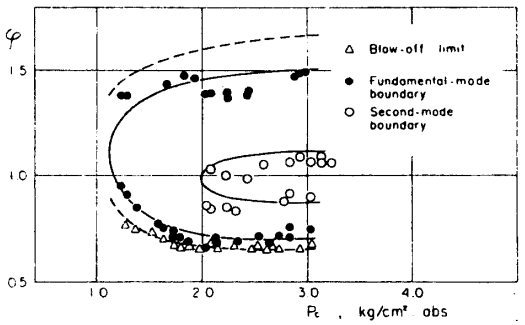

FIGURE 11. Instability regions: L_c=39.3 cm.

This document is provided by JAXA.

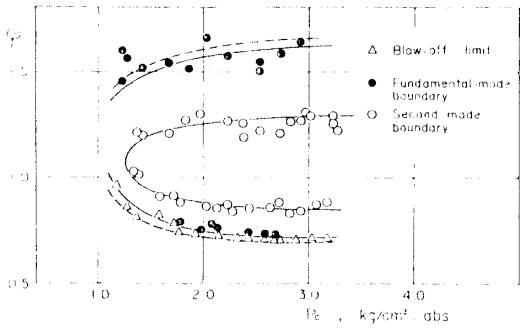

FIGURE 12. Instability regions: L_c=47.0 cm.

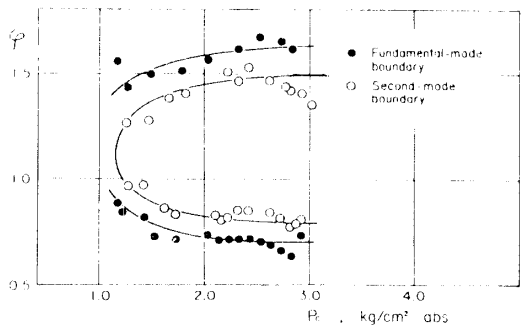

FIGURE 13. Instability regions: L_c=56.3 cm.

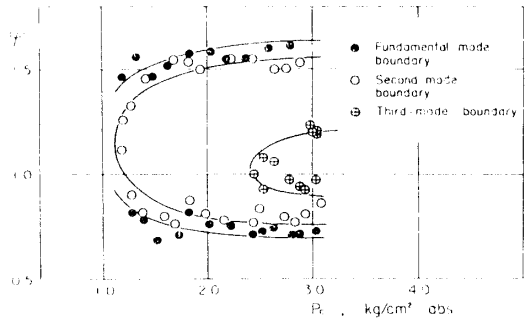

FIGURE 14. Instability regions: L_c=71.3 cm.

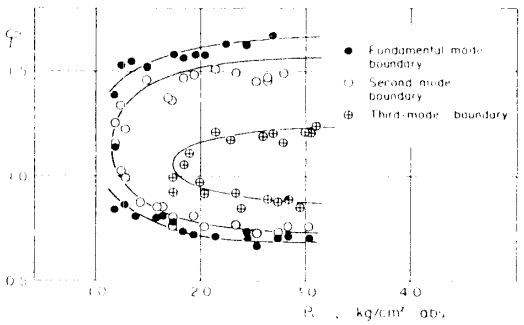

FIGURE 15. Instability regions: L_c=75.3 cm.

from 15.0 cm to 75.3 cm [*27*]. The instability regions were confirmed to exist always for any chamber length longer than 18.0 cm. In the case in which L_c was 15.0 cm, no organized oscillations appeared in the range of the chamber pressure observed in the present experiment, and only the steady combustion with turbulent flames stabilized at about 3～5 cm from the injector face was observed. In this case the pressure in the combustion chamber and the noise of the exhaust gas showed merely random fluctuations of small amplitudes as shown in Figure 16.

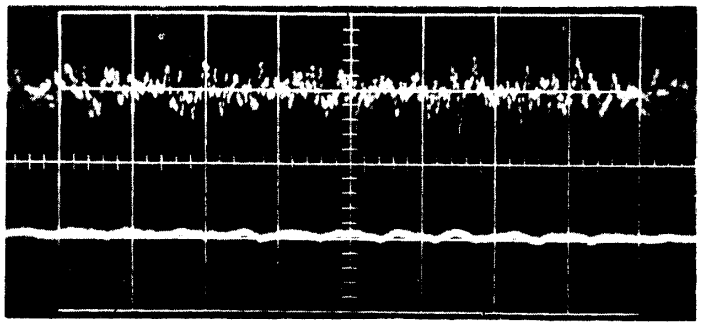

FIGURE 16. Pressure and noise traces of steady combustion: L_c=15.0 cm, P_c=2.55 kg/cm² abs.
upper: noise trace.
lower: pressure trace.

If the propellant equivalence ratio was decreased or increased at constant chamber pressure, the flames became to blow off at a certain value of φ and the combustion was not maintained over these limits.

This document is provided by JAXA.

In the case in which L_c was 19.5 cm, the fundamental-mode oscillations were observed near the stoichiometric mixture ratio of the propellant as shown in Figure 8, in which the instability boundary is presented by a solid line. For the chamber pressure of 3 kg/cm^2 abs, the length of about 18.0 cm may be considered to be the lower critical chamber length below which no high frequency combustion pressure oscillations of a longitudinal mode occur. If the oscillation occurred, the pressure trace and the noise trace showed the well-defined periodicity of same frequency as shown in Figure 17. With increasing the chamber length, the in-

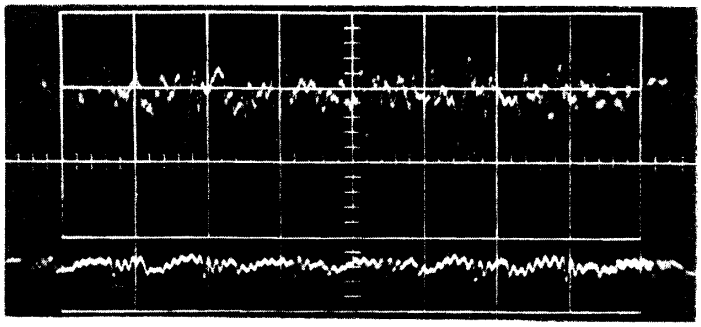

FIGURE 17. Pressure and noise traces of fundamental-mode oscillation: L_c=19.5 cm, P_c=3.50 kg/cm^2 abs.
upper: noise trace.
lower: pressure trace.

stability region of the fundamental-mode oscillations progressed steadily toward lower chamber pressure, extending its boundary both in rich and lean sides (Figures 9 and 10). The expansion of the instability boundary in rich side was larger than that in lean side. In these figures the blow-off limits are also presented by a dotted line. It seemed that the blow-off curve varied scarcely with increasing the chamber length and it was nearly parallel to P_c-axis at higher chamber pressure.

In the case in which L_c was 39.3 cm, the second harmonic-mode oscillations were observed inside the instability region of the fundamental-mode oscillations as shown in Figure 11. The instability region of the second harmonic-mode oscillations began to occur near the stoichiometric mixture ratio of the propellant just like that of the fundamental-mode oscillations (Figures 8 and 11). For the chamber pressure of 3 kg/cm^2 abs, the length of about 38.0 cm may be considered to be the lower critical chamber length for the second harmonic-mode oscillations. As the chamber length was increased further, the instability boundary of the fundamental-mode oscillations expanded still more and at the same time the instability region of the second harmonic-mode oscillations progressed steadily toward lower chamber pressure, extending its boundary both in rich and lean sides (Figures 11 and 12) just like that of the fundamental-mode oscillations already observed in the shorter combustion chambers (Figures 8, 9 and 10). If L_c was increased to 47.0 cm, however, the instability boundary of the fundamental-mode oscillations almost coincided with the blow-off curve of the flame both in rich and lean sides as shown in Figure 12. In the combustion chamber longer than this length, the steady combustion withut organized oscillation was scarcely observed

This document is provided by JAXA.

and the instability boundary of the fundamental-mode oscillations remained unchanged, being restricted by the blow-off curve, and only the instability region of the second harmonic-mode oscillations became larger as shown in Figure 13. As the result, the instability region of the fundamental-mode oscillations became smaller.

If L_c was increased to 66.0 cm, the third harmonic-mode oscillations were observed inside the instability region of the second harmonic-mode oscillations. Also the instability region of the third harmonic-mode oscillations began to occur near the stoichiometric mixture ratio of the propellant and progressed steadily toward lower chamber pressure, extending its boundary both in rich and lean sides as the chamber length was increased (Figures 14 and 15).

(*B*) *Oscillation frequency*

The frequency of each mode oscillation varied with the chamber length. Figure 18 shows the change of the observed periods of the oscillations as the chamber

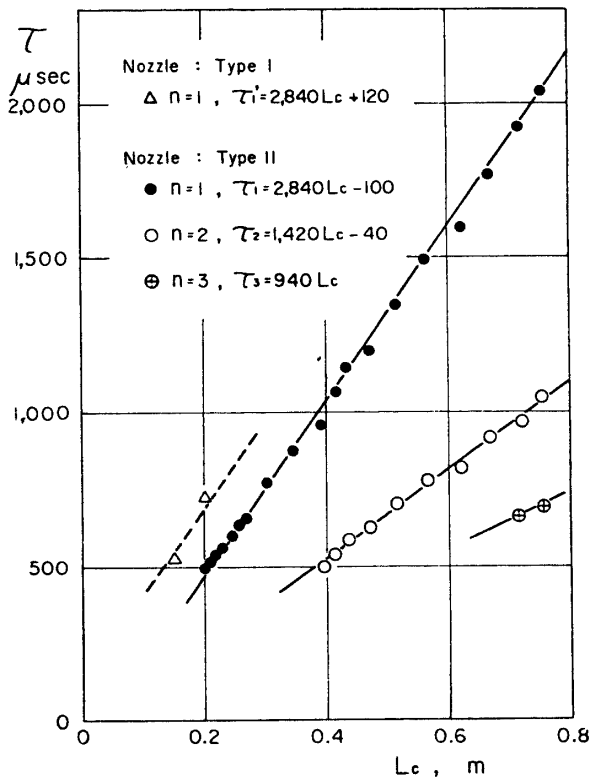

FIGURE 18. Period of pressure oscillations *vs.* combustion chamber length: T_c=1,600°K.

length was varied from 19.5 cm to 75.3 cm. In this paper the period is used instead of the frequency, because the period is found to be more essential parameter for the combustion oscillations. As will be discussed later, the period τ varies scarcely with the chamber pressure P_c, but considerably with the combustion gas temperature T_c. In Figure 18, the period τ observed for a constant gas tempera-

This document is provided by JAXA.

ture of 1,600°K is plotted against the chamber length.

As is well known, if the pressure oscillation is the acoustic mode in the combustion chamber with both ends closed, τ is given by the equation

$$\tau=\frac{2(L_c+\Delta L)}{nC_e} \tag{1}$$

in which ΔL, C_e and n are the end correction length of the nozzle, the effective sound velocity of the combustion gas and the positive integer giving the mode number of the oscillation, respectively. It is found that the observed results well satisfy the relation given by Equation (1) and the end correction length of the nozzle of Type II is very small.

III-3. Effect of the Chamber Pressure

In order to examine the effect of the mean combustion chamber pressure upon the longitudinal-mode pressure oscillations, the amplitudes and the periods of the pressure oscillations were plotted against the chamber pressure. Figure 19 presents the amplitudes of the pressure oscillations for the chamber length of 75.3 cm. Each group shows the observed amplitudes at a fixed combustion gas temperature (within ± 10°K). The increase in amplitude with the chamber pressure is found to be almost linear within the observed pressure range of the present experiment.

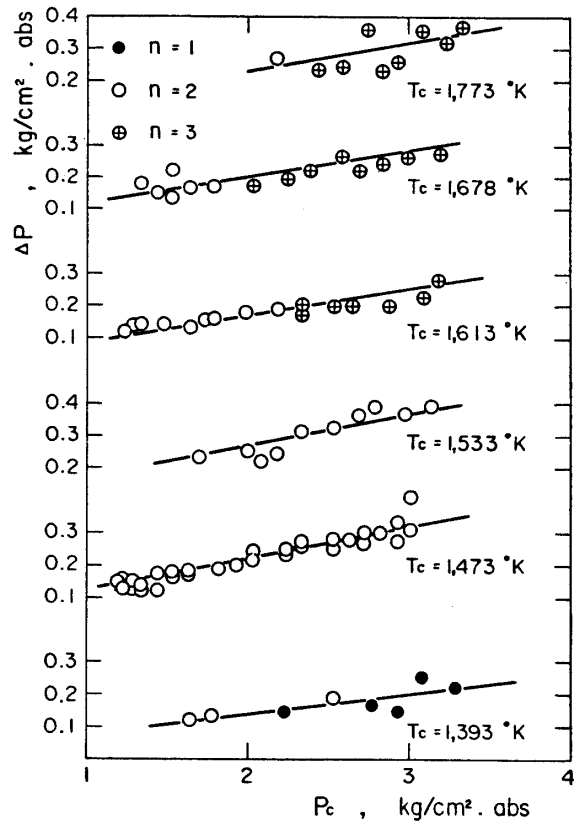

FIGURE 19. Amplitude of pressure oscillations *vs.* combustion chamber pressure: $L_c=75.3$ cm.

This document is provided by JAXA.

Although the accuracy of measurement on the absolute value of the amplitude was not so well, no remarkable effects of gas temperature upon the amplitude of the pressure oscillation were observed. The increase in amplitude with the chamber pressure can be attributed to the large amount of the feed energy to the oscillation in the case of the higher chamber pressure.

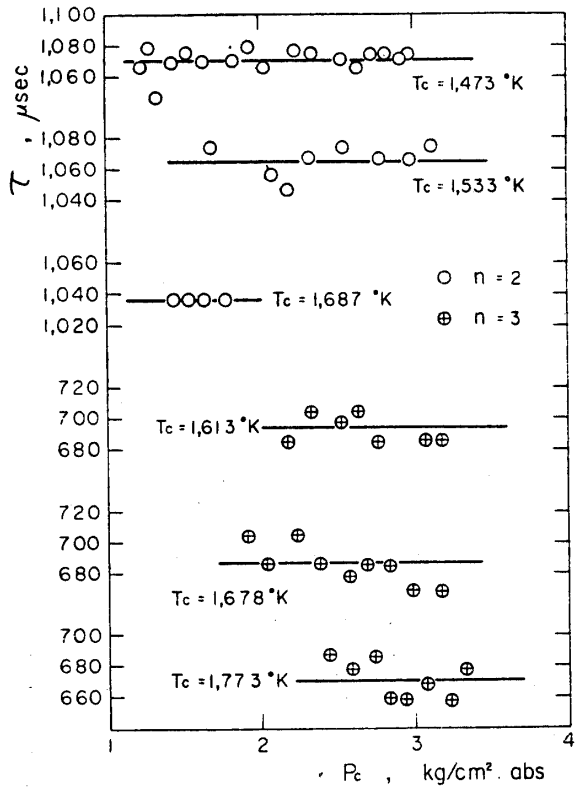

FIGURE 20. Period of pressure oscillations *vs.* combustion chamber pressure : L_c=75.3 cm.

Figure 20 illustrates the periods of the pressure oscillations as functions of the chamber pressure for the chamber length of 75.3 cm, the combustion gas temperature being the parameter. Although the periods of the oscillations show the tendency of a slight decrease with increasing chamber pressure, it may be considered that the period of the each mode oscillation is approximately constant independent of the chamber pressure in the case of constant gas temperature. K. Berman and S. H. Cheney, Jr. pointed out that the effect of the shock-type pressure oscillation was a slight increase in frequency, namely a slight decrease in period [*2*]. Also M. J. Zucrow and J. R. Osborn concluded from their experimental data that increasing the combustion chamber pressure increased the frequency of the combustion oscillations [*20*]. Within the pressure range observed in the present experiment however, this effect was not so remarkable.

This document is provided by JAXA.

III-4. Effect of the Combustion Gas Temperature

(A) *Relation between propellant equivalence ratio and combustion gas temperature*

If the combustion chamber was thermally insulated, the combustion gas temperature would be uniform in the combustion chamber and be the function of the propellant equivalence ratio φ only, independent of the flow rate of the mixture gas or the chamber pressure. In the present experiment, however, the water-cooled chamber was used, so that the temperature of the combustion gas stream had some distribution in the chamber, and the gas temperature T_c measured at a fixed location in the chamber was the function of φ and the chamber pressure.

Figure 21 presents the combustion gas temperature distributions along the x-axis of the chamber for three different values of φ in the case of a constant flow rate*.

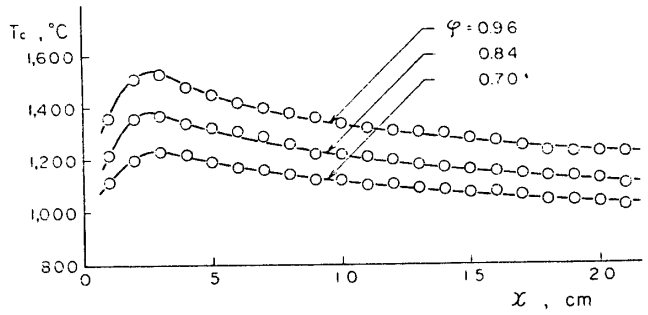

FIGURE 21. Combustion gas temperature distributions along the x-axis in the combustion chamber at atmospheric chamber pressure: L_c=22.5 cm.

These distributions were measured without the motor nozzle, that is, at atmospheric chamber pressure, but keeping the propellant injection velocity the same value as that in case when the nozzle was choked**. It is found that there exist considerable temperature gradients in the x-direction and that the reaction zone is located at about 3 cm from the injector face. Figure 22 shows an example of equitemperature lines in $P_c-\varphi$ diagram. It is found that T_c was affected appreciably also by the chamber pressure in the present experiment.

(B) *Oscillation frequency*

If the pressure oscillation is the acoustic mode, the oscillation period τ is given by

$$\tau=\frac{2(L_c+\Delta L)}{nC_e}\approx\frac{2L_c}{nC_e}, \qquad (2)$$

because the end correction length of the nozzle has already been found to be very small for the nozzle of Type II. For a particular chamber length, the frequency or the period of the oscillation depends on the sound velocity of the combustion gas, namely, on the gas temperature.

---

* The x-, y- and z-axes of the combustion chamber are illustrated in Figure 2.

** The propellant injection velocity was constant independent of the chamber pressure in the case when the nozzle was choked and was found to be about 120 m/sec.

This document is provided by JAXA.

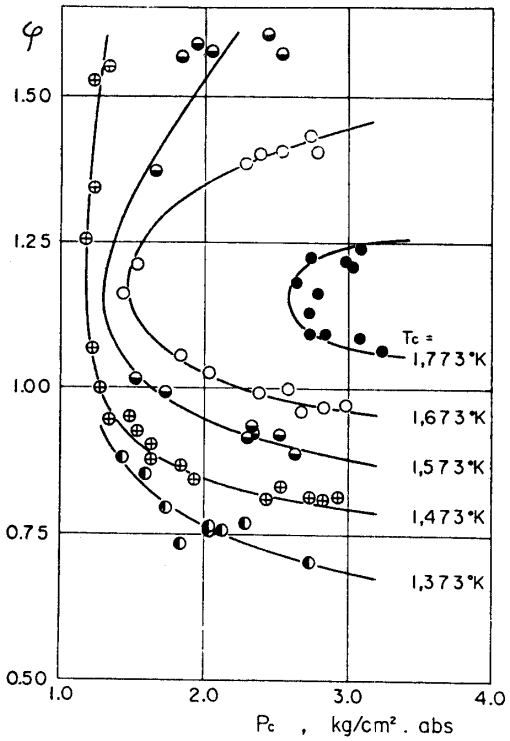

FIGURE 22. Equitemperature lines in P_c-φ diagram: L_c=75.3 cm.

As already pointed out, the combustion gas temperature was never uniform and had some distributions in the combustion chamber as shown in Figure 21. Consequently the sound velocity of the combustion gas is not constant in the chamber but decreases along the x-axis. Even in such a case, however, the effective average temperature T_e which will determine the period of the oscillation may be considered. If it is assumed that the average temperature T_e is proportional to the combustion gas temperature T_c measured at the fixed location in the chamber, the effective average sound velocity C_e of the combustion gas is given by the equation

$$C_e=\sqrt{\kappa gRT_e}=\sqrt{\kappa gRaT_c}\,, \tag{3}$$

in which

a: proportional constant$=T_e/T_c$,

κ: mean specific heat ratio of the combustion gas,

R: mean gas constant of the combustion gas, kg-m/kg-°K,

g: acceleration due to gravity, m/sec².

Substituting Equation (3) into Equation (2), we obtain

$$\tau=\frac{2L_c}{n\sqrt{a\kappa gRT_c}}$$

or

$$\log_{10}\tau=\log_{10}\frac{2L_c}{n\sqrt{a\kappa gR}}-\frac{1}{2}\log_{10}T_c\,. \tag{4}$$

This document is provided by JAXA.

In Equation (3), κ and R vary with φ, and κ is also the function of the gas temperature. However, these effects may be considered to be small, so that the first term in the right hand side of Equation (4) is regarded as a constant for a particular chamber length.

The observed periods of each mode oscillation are plotted against T_c in the logarithmic scales in Figure 23 for the chamber length of 75.3 cm. It is easily

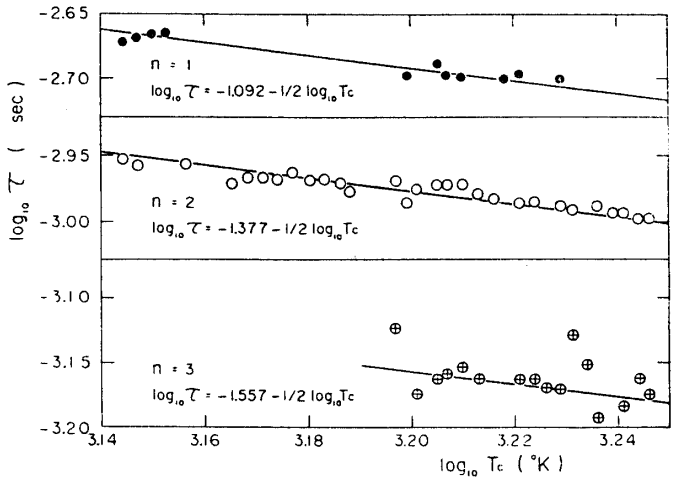

FIGURE 23. Period of pressure oscillations *vs.* combustion gas temperature: L_c=75.3 cm.

found that the observed periods of each mode oscillation well satisfy the relation given by Equation (4). Moreover, this result was also confirmed for any other chamber length. Therefore the values of the constant term of Equation (4) can be determined from the experimental results for each chamber length. Now we express the constant term of Equation (4) as $\log_{10} A$, then

$$\log_{10} A=\log_{10} L_c+\log_{10}\frac{2}{n}-\frac{1}{2}\log_{10}(a\kappa gR)\,. \qquad (5)$$

The values of $\log_{10} A$ determined from the experimental result are plotted against

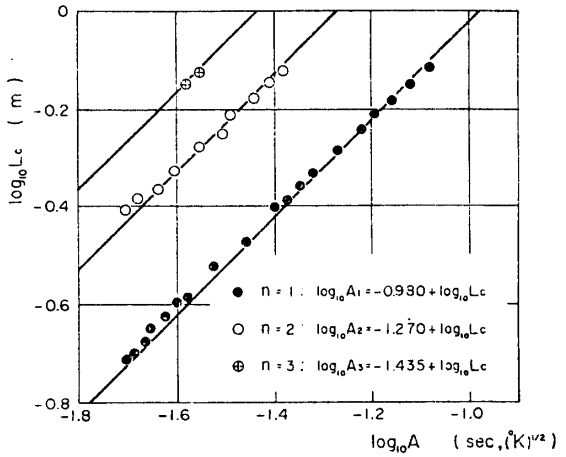

FIGURE 24. Parameter A *vs.* combustion chamber length.

This document is provided by JAXA.

$\log_{10} L_c$ in Figure 24. It is confirmed that $\log_{10} A$ increases linearly with $\log_{10} L_c$ as given by Equation (5). The values of $a\kappa gR$ can be calculated from Equation (5) and it is found that

$$a\kappa gR = 364.8 \text{ kg-m}^2/\text{kg-sec}^2\text{-}^\circ\text{K} \quad \text{for } n=1,$$
$$a\kappa gR = 346.7 \quad // \quad \text{for } n=2,$$
$$a\kappa gR = 329.6 \quad // \quad \text{for } n=3.$$

If we use the numerical values of 30.60 kg-m/kg°K for R (at $\varphi=1.0$) and 1.253 for κ (at $\varphi=1.0$ and $T=1{,}700^\circ$K), we find that

$$a=0.971 \quad \text{for } n=1,$$
$$a=0.923 \quad \text{for } n=2,$$
$$a=0.877 \quad \text{for } n=3.$$

III-5. Effect of Nozzle Shape

Some measurements were made with the nozzle of Type I in order to examine the effect of the nozzle shape upon the pressure oscillations. The observed periods of the pressure oscillations with this nozzle are plotted against the chamber length in Figure 18 as compared with that observed with nozzle of Type II. For a particular chamber length, the period of the oscillation with the nozzle of Type I is considerably larger than that with the nozzle of Type II. As easily understood, the difference may be attributed to the larger end correction length for the nozzle of Type I. Moreover, the wave forms of the pressure traces observed with this nozzle showed complex reflection at the entrance section of the nozzle.

IV. Discussion of Results

IV-1. The Characteristics of Pressure Oscillations

As already pointed out, in the case of lower chamber pressure, the smooth sinusoidal wave forms of the pressure oscillations with small amplitudes were observed. This indicates that the pressure oscillation is due to the standing wave of longitudinal mode. As the chamber pressure and the combustion gas temperature were increased, however, the amplitudes of the pressure oscillations were increased and finally the unique shock-type propagating pressure waves appeared. In the experiments of high frequency combustion oscillations in the liquid- and gaseous-propellant rocket motors, the presence of this shock-type propagating pressure wave has always been pointed out. In these experiments, however, the higher harmonic-mode longitudinal pressure oscillations have been scarcely observed except in some experiments in liquid-propellant rocket motors. It should be noteworthy that the propagating shock-type pressure waves of higher harmonic mode such as the second harmonic- and the third harmonic-modes were also observed in the present experiment.

In order to examine how the highr harmonic-mode pressure oscillations occurred in the combustion chamber, the pressure oscillations were measured at the same

This document is provided by JAXA.

time at three positions ($x=7.5$ cm, 31.0 cm and 41.0 cm) of the combustion chamber of 75.3 cm length. Figure 25 shows these pressure traces of each mode oscillation. For the synchroscope used in the present experiment, three pressure traces could not be recorded simultaneously. Therefore three different combinations of two simultaneous pressure traces are presented respectively for each mode oscillation in Figure 25. Small amplitudes of these pressure traces shown in this figure are due to the circumstances that the amplification of the signals in the synchroscope is comparatively low in the case when two signals are fed into it simultaneously. However, the actual amplitudes and the wave forms of the presure oscillations are the same as those presented in Figure 7. It was found from these pressure records that two and three shock-type pressure waves were propagating at the same time for the second harmonic- and the third harmonic-mode oscillations, respectively, and that these propagating waves were reflected respectively at the velocity nodes

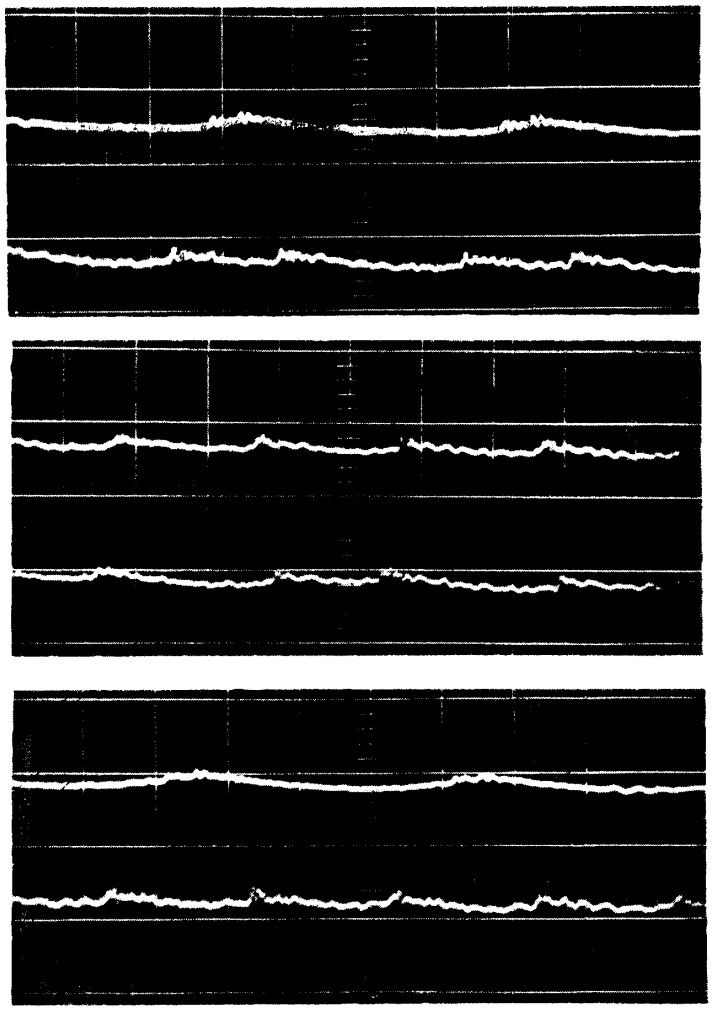

FIGURE 25. (A) Pressure traces of fundamental-mode, propagating shock-type waves observed simultaneously at two locations in the chamber.

1. upper: $x=7.5$ cm, lower: $x=31.0$ cm.
2. upper: $x=41.0$ cm, lower: $x=31.0$ cm.
3. upper: $x=7.5$ cm, lower: $x=41.0$ cm.

This document is provided by JAXA.

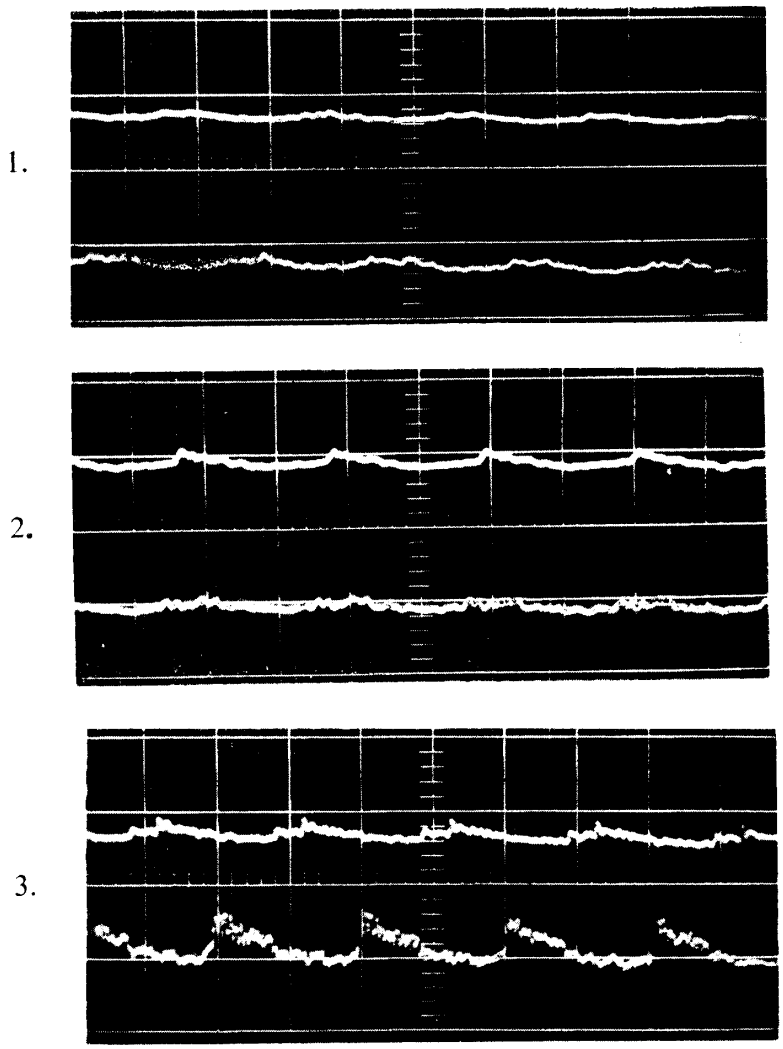

FIGURE 25. (B) Pressure traces of second harmonic-mode, propagating shock-type waves observed simultaneously at two locations in the chamber.

1. upper: $x = 7.5$ cm, lower: $x = 31.0$ cm.
2. upper: $x = 41.0$ cm, lower: $x = 31.0$ cm.
3. upper: $x = 7.5$ cm, lower: $x = 41.0$ cm.

This document is provided by JAXA.

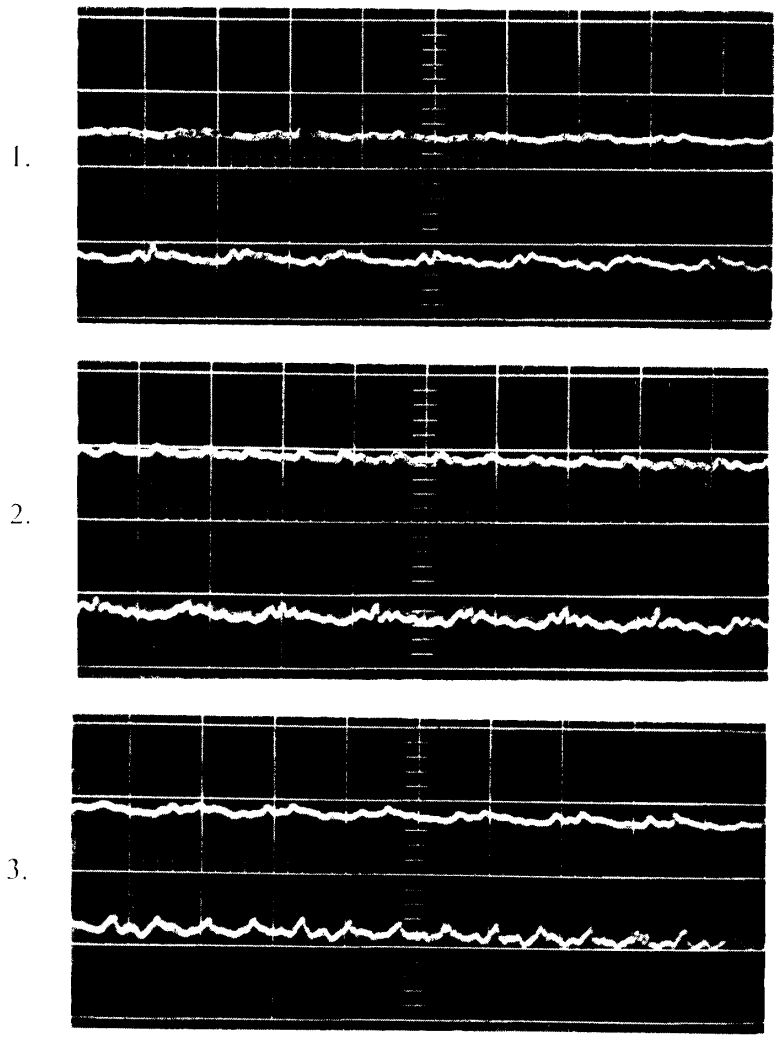

FIGURE 25. (C) Pressure traces of third harmonic-mode, propagating shock-type waves observed simultaneously at two locations in the chamber.

1. upper: x= 7.5cm, lower: x=31.0cm.
2. upper: x=41.0cm, lower: x=31.0cm.
3. upper: x= 7.5cm, lower: x=41.0cm.

of the higher harmonic standing waves in the combustion chamber. That is, for these propagating shock-type pressure waves, the phase relations shown in x-t (time) diagram in Figure 26 were confirmed.

It may be concluded from the above-mentioned characteristics of the pressure oscillations and the measured periods of oscillations that the pressure oscillations in the combustion chamber may be treated essentially as the standing waves of the longitudinal mode, though the shock-type pressure waves are propagating. If the pressure oscillation is due to the propagating shock wave, the wave propagating speed is not the sound velocity and Equation (1) does not hold precisely for such a type of pressure oscillation. However, if the shock propagating speed V_s is used in Equation (1) instead of the sound velocity C_s, the period of the oscillation may be considered to be given by Equation (1). In this case, the shock propa-

This document is provided by JAXA.

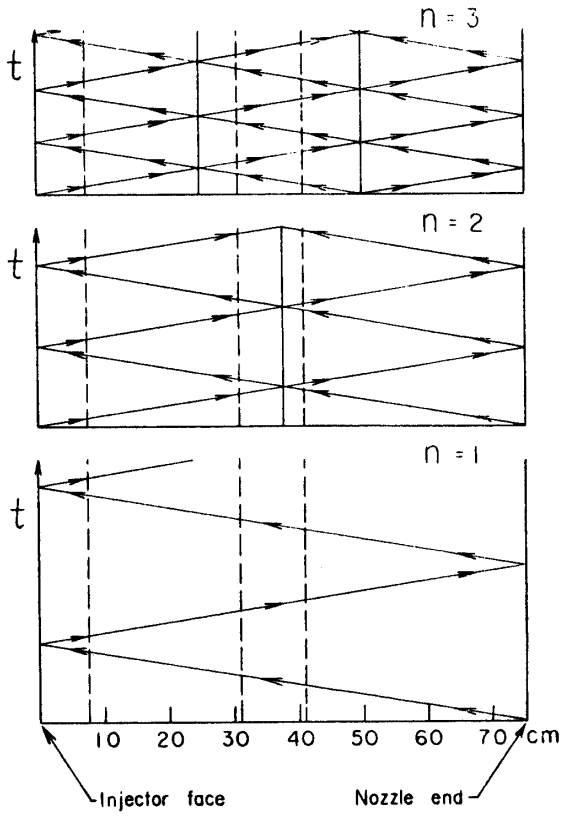

FIGURE 26. Phase relations of propagating shock-type pressure waves.

gating speed V_e is the product of the sound velocity C_e and the Mach number M of the shock wave, and M is determined by the shock strength P_2/P_1, in which P_1 and P_2 are the pressures before and behind the shock wave, respectively. The shock strength is the order of 1.1 in the present experiment and it may be the order of 1.5 at most even in actual rocket motor in which the mean chamber pressure is high enough and the observed amplitudes of the pressure oscillations are very large. According to the shock wave theory, Mach number of shock wave is about 1.04 and about 1.20 for the shock strength of 1.1 and 1.5, respectively. Therefore the effect of the shock strength, namely the amplitude of the shock-type pressure oscillation, upon the shock propagating speed is very small especially in the observed pressure range of the present experiment. In fact, as already pointed out in Figure 20, the observed periods of each mode oscillation show only a slight decrease with increasing the chamber pressure for constant gas temperature.

On the contrary, the combustion gas temperature has a considerable effect upon the oscillation period through the variation of the propagating speed of the pressure wave. As easily understood from the experimental results shown in Figure 23, however, it was confirmed that the effect of the combustion gas temperature upon Mach number of the shock-type pressure wave is very small and the combustion gas temperature has influence upon the oscillation frequency mainly through the variation of the sound velocity.

This document is provided by JAXA.

IV-2. Instability Regions

For the longitudinal-mode oscillations, the presence of the critical lower chamber length below which no organized oscillations appeared has always been pointed out in many experiments [2] [4] [20] [23]. In order to examine how the instability regions vary with the chamber length, the instability boundaries were replotted in L_c-φ diagram for a fixed chamber pressure. Figure 27 presents the instability boundaries in the case of $P_c=3\,\mathrm{kg/cm^2}$ abs. In this case, the lower critical chamber lengths are found to be about 18.0 cm, 38.0 cm and 66.0 cm for the fundamental-, the second harmonic- and the third harmonic-mode oscillations, respectively. The periods of oscillations of each mode corresponding to these critical chamber lengths are about the same value and are approximately 500 μsec. This suggests that the initiation of combustion oscillations may be governed essentially by the period of oscillation rather than the chamber length. Therefore the instability boundaries shown in Figure 27 are replotted in $\tau-\varphi$ diagram as shown in Figure 28, in which τ is the period of oscillation. It is found that the instability

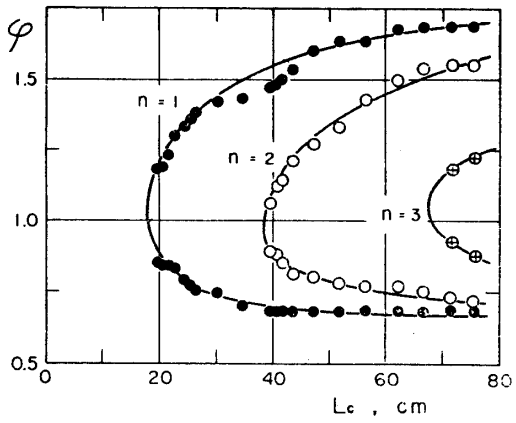

FIGURE 27. Instability regions: $P_c=3\,\mathrm{kg/cm^2}$ abs.

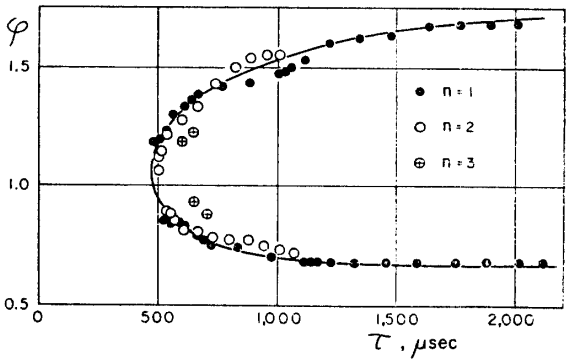

FIGURE 28. Instability regions: $P_c=3\,\mathrm{kg/cm^2}$ abs.

boundaries for the fundamental-, the second harmonic- and the third harmonic-mode oscillations are all expressed as one curve for a given injector and a fixed chamber pressure.

The important results of the instability regions are that the organized oscillation

This document is provided by JAXA.

of smaller period than the critical value did not occur in the combustion chamber and that the critical value which is the function of φ was about the same for each mode oscillation in the case of constant chamber pressure. From these experimental results, the initiation of the combustion oscillations of the fundamental- and the higher harminic-modes may be explained qualitatively by the following consideration. It is assumed that there is a combustion time lag or a response time which may be thought to be the total time required to produce an increase in heat release rate in the reaction zone through some mechanical and chemical processes and to feed the additional energy to the pressure wave necessary to sustain the oscillation after the injected propellants are affected by the pressure wave propagating to the injector face. This time lag is determined in general by the fuel composition, the chamber pressure, the equivalence ratio and the injection velocity of the propellant, etc., and it is considered to be composed of the mechanical time lag and the chemical time lag. In the case of constant injection velocity, this time lag is the function of φ and P_c. If the oscillation period determined by the chamber length and the combustion gas temperature, etc. is smaller than the assumed combustion time lag, the pressure wave propagating to the injector face can not receive the additional energy induced by the preceeding pressure wave. As the result, the pressure wave will decay and the combustion oscillations will not be sustained. Therefore it may be reasonable to consider that the critical values of the oscillation periods shown in Figure 28 indicate the combustion time lag itself and that the period of oscillation must be larger than this critical combustion time lag τ_{cr} in order the combustion oscillations to be sustained, namely the combustion can occur only when the criterion,

$$\tau \geq \tau_{cr}, \tag{6}$$

is satisfied.

In the first place, let us consider the case in which P_c is constant and the chamber length L_c is varied. The critical combustion time lag τ_{cr} for a given value of the chamber pressure is assumed to be given as a function of φ, being restricted by the blow-off limits, as shown in Figure 29. On the other hand, the period τ of the pressure oscillation which can occur in the combustion chamber of length L_c is

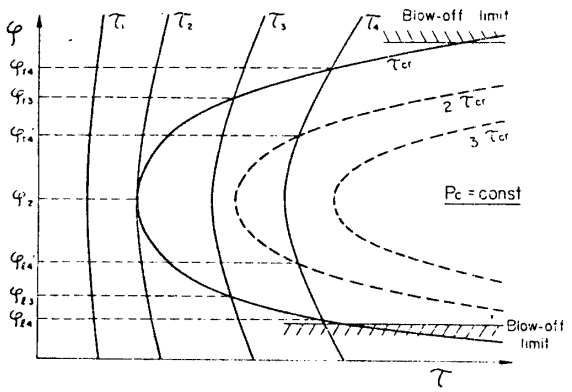

FIGURE 29. Combustion time lag: P_c=const.

This document is provided by JAXA.

determined by the relation,

$$\tau=\frac{2L_c}{nMC_e}. \tag{7}$$

τ increases with L_c according to this relation. In the case of a short chamber length L_{c1}, the period τ_1 corresponding to this chamber length is also small and the criterion (6) is not satisfied for any values of φ. Consequently any combustion oscillation does not occur. If the chamber length is increased to L_{c2} and the period of the fundamental-mode oscillation becomes τ_2, the criterion (6) is satisfied at φ_2, so that the fundamental-mode oscillation may occur only for this equivalence ratio φ_2. Namely, L_{c2} corresponds to the so-called critical lower chamber length for a given chamber pressure. For a larger chamber length L_{c3}, the period τ_3 of the fundamental-mode oscillation corresponding to this chamber length satisfies the criterion (6) in the range of φ between φ_{r3} and φ_{l3} and therefore the fundamental-mode oscillation will occur in this range of φ. As the chamber length is increased and then the period of the fundamental-mode oscillation increases, the instability range of φ becomes larger. However, if the period of the fundamental-mode oscillation becomes larger than $2\tau_{cr}$, the period of the second harmonic-mode oscillation also becomes to satisfy the criterion (6). For example, if the period of the fundamental-mode oscillation is τ_4, the fundamental-mode oscillation is possible to occur in the range of φ between φ_{r4} and φ_{l4}, and at the same time the second harmonic-mode oscillation is possible to occur in the range of φ between φ'_{r4} and φ'_{l4}. Namely, both the fundamental- and the second harmonic-mode oscillations are possible to occur in the range of φ between φ'_{r4} and φ'_{l4}. In such a case, however, the higher harmonic-mode oscillation, namely the oscillation of the mode of smaller period is considered to be ready to occur. Similarly, if the chamber length is large enough and the period of the fundamental-mode oscillation becomes larger than $3\tau_{cr}$, the third harmonic-mode oscillation may be considered to occur. Therefore it is easily understood that the period of the combustion oscillation which may occur actually in the combustion chamber is limited to the range of τ between $\tau_{cr}(\varphi)$ and $2\tau_{cr}(\varphi)$.

In the next place, let us consider the case in which L_c is constant and P_c is varied. In this case, the periods of the fundamental- and the higher harmonic-mode pressure oscillations which will occur in the combustion chamber are determined by the relation (7) as the function of φ as shown in Figure 30, in which τ_L', τ_L'' and τ_L''' are the periods of the fundamental-, the second harmonic- and the third harmonic-mode oscillations, respectively. Also in this case, the critical combustion time lag τ_{cr} is assumed to be given as a function of φ, being restricted by the blow-off limits, as shown in Figure 30, and moreover, this time lag is assumed to become smaller with increasing the chamber pressure as shown in Figure 30.

In the case of a low chamber pressure P_{c1}, the critical combustion time lag τ_{cr} corresponding to this chamber pressure is large and the criterion (6) is not satisfied for any value of φ. Consequently any combustion oscillation does not occur in

This document is provided by JAXA.

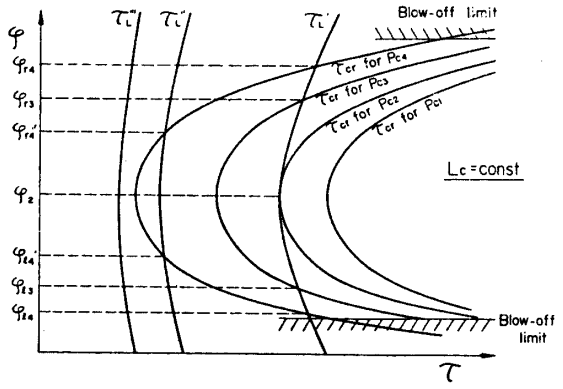

FIGURE 30. Combustion time lag: L_c=const.

this chamber pressure. If the chamber pressure is increased to P_{c2}, the criterion (6) is satisfied at φ_2 for the fundamental-mode oscillation, so that the fundamental-mode oscillation may occur only for this equivalence ratio φ_2. For a higher chamber pressure P_{c3}, the period of the fundamental-mode oscillation becomes larger than τ_{cr} in the range of φ between φ_{r3} and φ_{l3}, and therefore the fundamental mode oscillation will occur in this range of φ. As the chamber pressure is increased, the instability region becomes larger. At the same time, however, the period of the second harmonic-mode oscillation becomes also to satisfy the criterion (6). For example, if the chamber pressure becomes P_{c4}, the fundamental-mode oscillation is possible to occur in the range of φ between φ_{r4} and φ_{l4}, and at the same time the second harmonic-mode oscillation is possible to occur in the range of φ between φ'_{r4} and φ'_{l4}. Namely, both the fundamental- and the secon harmonic-mode oscillations are possible in the range of φ between φ'_{r4} and φ'_{l4}. In such a case, however, the higher harmonic-mode oscillation is considered to be ready to occur. Similarly, if the chamber pressure becomes high enough and the critical combustion time lag becomes smaller than τ'''_L, the third harmonic-mode oscillation may be considered to occur.

It is found that the considerations mentioned above can explain the experimental results of the instability boundaries shown in Figures 8～15 without contradiction. However, the essential features of the critical combustion time lag assumed in the above considerations are not yet elucidated at the present experimental situation and it is emphasized that the further study of this combustion time lag is necessary in order the mechanism of the high frequency combustion oscillations to be made clear.

V. CONCLUSIONS

The experimental investigations of the high frequency combustion oscillations in a rocket motor burning premixed gases as propellants have led to the following conclusions.

(1) Although the propagating shock-type pressure wave appears as the feed energy to the oscillation is increased, the high frequency pressure oscillations in

This document is provided by JAXA.

the combustion chamber may be treated essentially as the standing wave of the longitudinal mode, because the second harmonic- and the third harmonic-mode pressure oscillations were obsrved in the combustion chamber, i.e., two and three shock-type pressure waves were propagating at the same time for the second harmonic- and the third harmonic-mode oscillations, respectively, and moreover the measured periods of each mode oscillation satisfy the relation for the acoustic-mode oscillations.

(2) The effect of the chamber pressure upon the shock propagating speed is very small in the observed pressure range and the period of the oscillation decreases slightly with increasing the chamber pressure. On the other hand, however, the combustion gas temperature has a considerable effect upon the period of the oscillation through the variation of the sound velocity of the combustion gas.

(3) By assuming the existence of some critical combustion time lag for the combustion oscillations, the experimental results on the limits of initiation of each mode pressure oscillation could be explained without contradiction.

By the present experiment, the essential features of the high frequency combustion pressure oscillations occurred actually in the combustion chamber could be well elucidated, and these experimental results are thought to be very useful for the theoretical analysis of the high frequency combustion oscillations. On the other hand, however, the sustaining mechanism of the combustion oscillations is not yet fully understood and the further experiments are now being conducted, and the detailed discussion on the sustaining mechanism will be presented in the following paper.

The authors would like to express their sincere thanks to Messers. T. Okano, M. Hori and I. Yamaoka for their active cooperation in conducting the experiments. This work is supported partly by the fund of the Ministry of Education in Aid of Scientific Research.

Department of Jet Propulsion
Aeronautical Research Institute
University of Tokyo, Tokyo.
March 10, 1964.

References

[1] K. Berman and S. E. Logan: Combustion studies with a rocket motor having a full-length observation window, Journ. American Rocket Soc., Vol. 22, No. 2 (1952), pp. 78/85 and 103.

[2] K. Berman and S. H. Cheney, Jr.: Combustion studies in rocket motors, Journ. American Rocket Soc., Vol. 23, No. 2 (1953), pp. 89/96 and 98.

[3] K. Berman and S. H. Cheney, Jr.: Rocket motor instability studies, Jet Propulsion, Vol. 25, No. 10 (1955), pp. 513/518.

[4] H. Ellis, I. Odgers, A. J. Stosick, N. Van de Verg and R. S. Wick: Experimental investigation of combustion instability in rocket motors, Fourth Intern. Symp. on Combustion, Williams and Wilkins Co., Baltimore (1953), pp. 880/885.

[5] P. B. Lawhead: Photographic studies of combustion processes in liquid propellant rockets, Eighth Intern. Symp. on Combustion, Williams and Wilkins Co., Baltimore (1962), pp.

This document is provided by JAXA.

1140/1151.
[6] L. Crocco and S. I. Cheng: Theory of combustion instability in liquid propellant rocket motors, AGARDGRAPH No. 8, Butterworths Sci. Publications, London (1956).
[7] L. Crocco, J. Grey and D. T. Harrje: Theory of liquid propellant rocket combustion instability and its experimental verification, ARS Journ., Vol. 30, No. 2 (1960), pp. 159/168.
[8] F. E. C. Culick: Stability of high frequency pressure oscillations in rocket combustion chambers, AIAA Journ., Vol. 1, No. 5 (1963), pp. 1097/1104.
[9] Lewis Laboratory Staff: A summary of preliminary investigations into the characteristics of combustion screech in ducted burners, NACA Report 1384 (1954).
[10] A. A. Putnam and W. R. Dennis: A study of burner oscillations of the organ-pipe type, Trans. ASME, Vol. 75 (1953), pp. 15/28.
[11] A. A. Putnam and W. R. Dennis: Organ-pipe oscillations in a flame-filled tube, Fourth Intern. Symp. on Combustion, Williams and Wilkins Co., Baltimore (1953), pp. 566/575.
[12] A. A. Putnam and W. R. Dennis: Burner oscillations of the gauge-tone type, Journ. Acoust. Soc. Amer., Vol. 26, No. 5 (1954), pp. 716/725.
[13] A. A. Putnam and W. R. Dennis: Suppression of burner oscillations by acoustical dampers, Trans. ASME, Vol. 77 (1955), pp. 875/883.
[14] A. A. Putnam and W. R. Dennis: Organ-pipe oscillations in a burner with deep ports, Journ. Acoust. Soc. Amer., Vol. 28, No. 2 (1956), pp. 260/269.
[15] H. J. Merk: Analysis of heat-driven oscillations of gas flows, I. General considerations, Appl. Sci. Res., A, Vol. 6 (1957), pp. 317/336.
[16] H. J. Merk: Analysis of heat-driven oscillations of gas flows, II. On the mechanism of the Rijke-tube phenomenon, Appl. Sci. Res., A, Vol. 6 (1957), pp. 402/420.
[17] H. J. Merk: Analysis of heat-driven oscillations of gas flows, III. Characteristic equation for flame-driven oscillations of the organ-pipe type, Appl. Sci. Res., A, Vol. 7 (1958), pp. 175/191.
[18] H. J. Merk: Analysis of heat-driven oscillations of gas flows, IV. Discussion of the theoretical results concerning flame-driven oscillations, Appl. Sci. Res., A, Vol. 7 (1958), pp. 192/204.
[19] H. J. Merk: Analysis of heat-driven oscillations of gas flows, V. Influence of heat transfer in the burner ports on the stability of combustion of premixed gases, Appl. Sci. Res., A, Vol. 8 (1959), pp. 1/27.
[20] M. J. Zucrow and J. R. Osborn: An experimental study of high-frequency combustion pressure oscillations, Jet Propulsion, Vol. 28, No. 10 (1958), pp. 654/659.
[21] M. J. Zucrow, J. R. Osborn and A. C. Pinchak: Luminosity and pressure oscillations observed with longitudinal and transverse modes of combustion instability, ARS Journ., Vol. 30, No. 8 (1960), pp. 758/761.
[22] J. R. Osborn and J. M. Bonnel: Importance of combustion chamber geometry in high frequency oscillations in rocket motors, ARS Journ., Vol. 31, No. 4 (1961), pp. 482/486.
[23] J. R. Osborn and J. M. Bonnel: Effect of fuel composition on high frequency oscillations in rocket motors burning premixed hydrocarbon gases and air, ARS Journ., Vol. 31, No. 10 (1961), pp. 1397/1401.
[24] J. R. Osborn and R. L. Derr: An experimental investigation of longitudinal combustion pressure oscillations, Jet Propulsion Center, Purdue Univ., Report No. I-62-8 (1962).
[25] K. Yamazaki and H. Tsuji: An experimental investigation on the stability of turbulent burner flames, Eighth Intern. Symp. on Combustion, Williams and Wilkins Co., Baltimore (1962), pp. 543/553.
[26] H. Tsuji and T. Okano: Flame stabilization by a bluff-body flameholder with gas ejection, Aero. Res. Inst., Univ. of Tokyo, Report No. 369 (1962).
[27] T. Takeno: Experimental investigations on high-frequency combustion oscillations, Master Thesis, Graduate School of Aero. Eng., Univ. of Tokyo (1963).

This document is provided by JAXA.